RADIO SCIENCE, VOL. 44, RS0A19, doi:10.1029/2008RS004075, 2009

Investigations into the feasibility of multiple input multiple output techniques within the HF band: Preliminary results

S. D. Gunashekar,[1] E. M. Warrington,[1] S. Salous,[2] S. M. Feeney,[2] N. M. Abbasi,[1] L. Bertel,[3] D. Lemur,[3] and M. Oger[3]

Received 31 October 2008; revised 25 April 2009; accepted 26 May 2009; published 5 August 2009.

[1] The concept of multiple input multiple output (MIMO) has become a productive area of research in the field of wireless communications with the aim of delivering increased data throughput. However, to date, MIMO research has focused primarily on short-range communications within the VHF, UHF, and SHF bands, and very little research has been conducted toward exploiting MIMO techniques for long-range communications within the HF band. Between September 2007 and September 2008, several experimental campaigns were conducted to investigate the feasibility of applying MIMO techniques within the HF band. The results of measurements over a 255 km path from Durham to Leicester within the United Kingdom are presented in this paper with particular emphasis on the use of heterogeneous antenna arrays at the transmitter and receiver.

Citation: Gunashekar, S. D., E. M. Warrington, S. Salous, S. M. Feeney, N. M. Abbasi, L. Bertel, D. Lemur, and M. Oger (2009), Investigations into the feasibility of multiple input multiple output techniques within the HF band: Preliminary results, *Radio Sci.*, *44*, RS0A19, doi:10.1029/2008RS004075.

1. Introduction

[2] Multiple input multiple output (MIMO) systems employ antenna arrays at both the transmitter and receiver. It is well known that MIMO systems can improve the spectral efficiency of communication links by providing substantial increases in data rates without increased bandwidth [*Foschini*, 1996; *Shiu et al.*, 2000; *Gesbert et al.*, 2002; *Lim et al.*, 2007]. For MIMO to be successful, a rich fading or scattering environment is required which, in effect, facilitates the creation of a number of parallel channels that carry different data streams. Under ideal conditions, the channel capacity can increase linearly with the lower of the number of transmit/receive antennas. Therefore, in contrast to traditional techniques such as diversity that mitigate the effects of fading, MIMO systems exploit the presence of multipath to enhance the channel capacity. Furthermore, the more decorrelated the signals are between the individual antenna elements at both ends of the link, the greater is the advantage obtained. To date, MIMO research has focused primarily on short-range wireless communications within the VHF band and above [*Foschini*, 1996; *Shiu et al.*, 2000; *Gesbert et al.*, 2002; *Lim et al.*, 2007] and has not been widely addressed in the lower-frequency bands.

[3] At HF (3–30 MHz), radio waves are capable of traveling well beyond line of sight by means of reflections from the ionosphere. These paths may be either single hop or multiple hop reflections from the different ionospheric regions (the *E* region and/or the *F* region). Additionally, because of the presence of the earth's magnetic field, each incident radio wave splits into two electromagnetic components known as the ordinary (*O*) and the extraordinary (*X*) modes. The two magnetoionic components take different paths through the ionosphere and arrive at the receiver as elliptically polarized signals with opposite rotational sense. The actual number of multipath components connecting a transmitter to a receiver depends on the geometry of the radio link, the frequency of operation, the time of day, season, geomagnetic activity and sunspot number. Therefore, an HF propagation path through the ionosphere is prone to extensive fading as a consequence of time variant multipath and multimode propagation. Consequently, it would appear that the use of HF signals in a multielement transmitter-receiver system would be an ideal candidate for a MIMO system. So far, however, apart from the research outlined by *Xu et al.* [2004], *Brine et al.* [2006], and *Strangeways* [2006], there has been no

[1]Department of Engineering, University of Leicester, Leicester, UK.
[2]School of Engineering, Durham University, Durham, UK.
[3]IETR, UMR6164, Université de Rennes 1, CNRS, Rennes, France.

0048-6604/09/2008RS004075$11.00

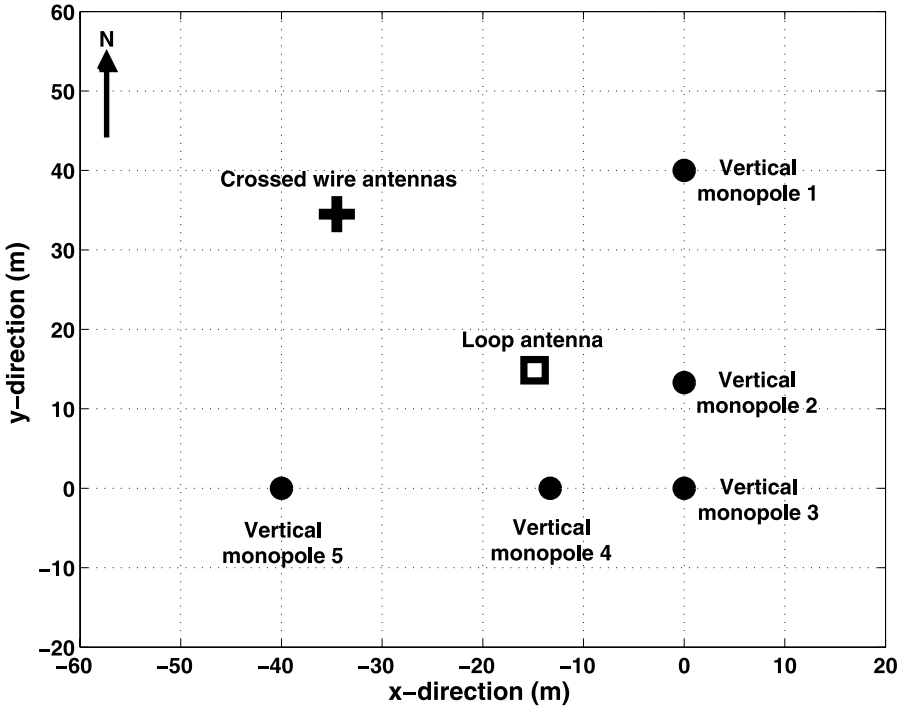

Figure 1. The relative positions of the antennas employed in the receiving antenna array in Bruntingthorpe (near Leicester, United Kingdom) during several of the experimental campaigns.

experimental or modeling research conducted in this area.

[4] Between September 2007 and September 2008, the authors undertook a number of experimental campaigns to investigate the feasibility of applying MIMO techniques within the HF band [*Gunashekar et al.*, 2008; *Salous et al.*, 2008]. This paper discusses some of the significant results that have been obtained in this study with particular emphasis on the use of heterogeneous antenna arrays at the transmitter and receiver. (A heterogeneous antenna array is one that is composed of either different types of antennas, or the same types of antennas with different orientations, while a homogeneous antenna array is one that is composed of identical antennas with the same orientation.)

2. Experimental Arrangement

[5] For the investigations carried out in this study, a purpose-built multichannel transmitter system and multichannel receiver system was implemented. The receiver site was located in Bruntingthorpe (near Leicester), United Kingdom, and the transmitter site in Durham, United Kingdom, giving an approximately N-S path with a range of 255 km. Currently, the system has the capability of transmitting on up to four antennas and receiving on up to eight antennas. In order to examine the effects of antenna heterogeneity at the transmitter, a variety of antennas were used in the measurement campaigns (e.g., vertical, loop, dipole and crossed wire antennas). At the receiver, a spaced antenna array (an L-shaped array of five vertical monopole antennas) was employed in several of the campaigns so that the effect of antenna spacing could be determined. The array consisted of a 40 m long N-S arm (pointing in the general direction of Durham) and a 40 m long E-W arm (see Figure 1). The two orthogonal arms of this configuration facilitated the examination of any orientation-dependent propagation effects. In some of the campaigns, additional antennas (e.g., loops and crossed wires) were also utilized to introduce heterogeneity at the receiver. More recently, the feasibility of deploying compact, colocated, heterogeneous antenna arrays at the receiver has also been investigated.

3. Measurements and Analysis

[6] Sections 3.1 and 3.2 provide examples of cases in which different antenna configurations were employed. In all the campaigns, data were collected over a period of

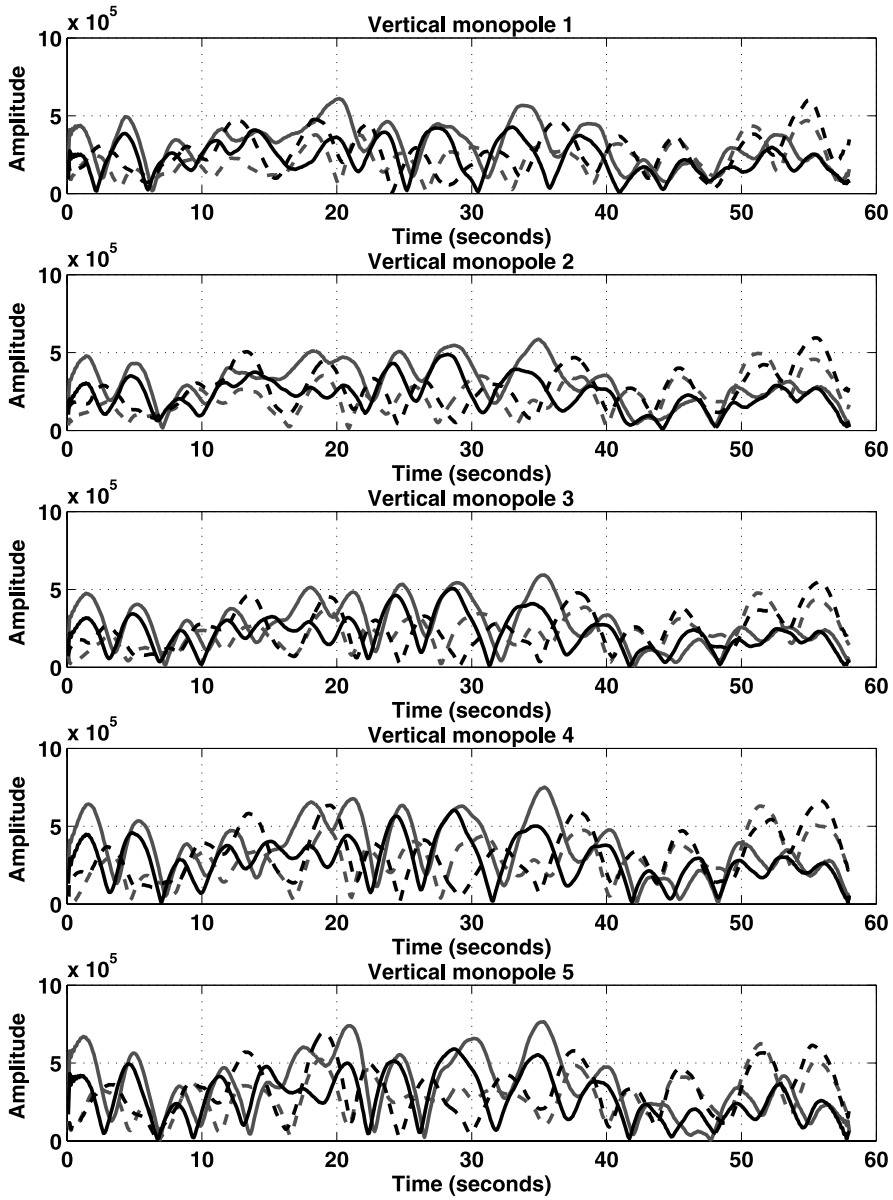

Figure 2. Amplitude patterns (linear units) observed for a period of approximately 1 min on the five elements of the L-shaped vertical monopole antenna array in Bruntingthorpe at 1602 UT on 2 November 2007 for four CW signals (with successive offsets of 10 Hz) transmitted from Durham using four separate antennas. Dashed gray line is the E-W arm of crossed wire array 1 (TX-1; 5.255010 MHz), solid gray line is the N-S arm of crossed wire array 1 (TX-2; 5.255020 MHz), dashed black line is the E-W arm of crossed wire array 2 (TX-3; 5.255030 MHz), and solid black line is the N-S arm of crossed wire array 2 (TX-4; 5.255040 MHz).

few hours (in blocks of approximately 1-min duration), and the specific examples presented in sections 3.1 and 3.2 are representative of the majority of the measurements.

[7] Concurrent measurements of the amplitude of CW signals received from the various transmitting antennas were made at each of the receiving antennas. For the various transmit antennas, slightly different frequencies

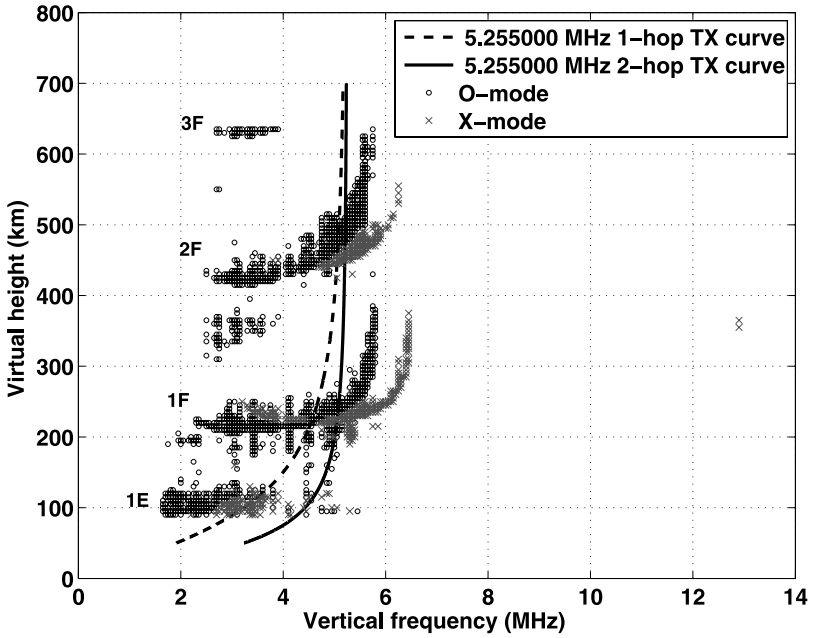

Figure 3. Vertical ionogram observed at the Chilton ionosonde station superimposed by transmission curves (5.255 MHz) for the Durham-Bruntingthorpe path at 1600 UT on 2 November 2007.

(offset by 10–20 Hz) were used. During testing, it was verified that the slightly different frequencies exhibited identical fading when transmitted simultaneously on a single antenna. This result confirmed that the differences in frequencies (when used on separate transmit antennas) would not contribute to any kind of decorrelation during the MIMO campaigns. It must be noted that in the current MIMO setup, the frequency offsets were required solely to identify the specific transmit antenna signal sources, and will not be needed in operational MIMO systems that will be implemented in the future (see section 4).

3.1. The 4 × 8 MIMO Configuration (2 November 2007)

[8] A 4 × 8 MIMO link (four transmitting antennas and eight receiving antennas) using a nominal transmission frequency of 5.2550 MHz was set up. For the transmit array, two pairs of orthogonally oriented inverted "V" wire antennas spaced approximately 22 m apart (center-to-center distance) were employed with the following specifications: E-W arm of crossed wire array 1 (TX-1; 5.255010 MHz), N-S arm of crossed wire array 1 (TX-2; 5.255020 MHz), E-W arm of crossed wire array 2 (TX-3; 5.255030 MHz), and N-S arm of crossed wire array 2 (TX-4; 5.255040 MHz). Each pair of inverted V antennas was supported by its own mast and the orthogonal wires comprising each pair were crossed at the same point on their respective masts (approximately 9 m above ground level). The N-S arms of the two crossed wire antennas were oriented in such a way that they were pointing toward the receiving site (bearing is 173°).

[9] For the receive array of Figure 1, in addition to the L-shaped configuration of five vertical monopoles (RX-1–RX-5), a square loop antenna (side length ∼1.5 m; E-W orientation) (RX-6) and a pair of orthogonally oriented inverted V antennas (RX-7, RX-8) were set up. Both the inverted V antennas (wire length ∼32 m) were supported by the same mast and were crossed at the same point on the mast (approximately 7.6 m above ground level). The N-S arm of the receiver crossed wire antenna was pointing in the general direction of Durham. Note that the orientations of the loop and inverted V antennas are specified as the plane containing the antenna elements.

3.1.1. Structure of the Ionosphere and Fading

[10] For the majority of the data recorded, the amplitude patterns across the eight receiving antennas indicated deep fading for all four transmissions. As an example, the amplitude pattern across the five monopoles of the L-shaped array for CW signals received from Durham for a period of approximately 1-min (at 1602 UT on 2 November 2007) is depicted in Figure 2. The four simultaneously transmitted carrier signals were recovered at each receiving antenna after applying a filtering procedure. When transmission curves were superimposed on the corresponding vertical ionogram obtained

Table 1. Magnitudes of Amplitude Correlation Coefficients Between the Various Transmissions at Each Receiving Antenna for a 60 s Data File Collected at 1602 UT on 2 November 2007[a]

	Magnitude of Amplitude Correlation Coefficients					
	[TX-1, TX-2]	[TX-1, TX-3]	[TX-1, TX-4]	[TX-2, TX-3]	[TX-2, TX-4]	[TX-3, TX-4]
RX-1	0.15	0.63	0.35	0.07	0.72	0.08
RX-2	0.20	0.72	0.22	0.14	0.77	0.08
RX-3	0.15	0.69	0.22	0.31	0.74	0.29
RX-4	0.18	0.71	0.28	0.29	0.73	0.33
RX-5	0.27	0.81	0.28	0.26	0.74	0.25
RX-6	0.28	0.52	0.26	0.17	0.80	0.18
RX-7	0.14	0.61	0.07	0.40	0.81	0.33
RX-8	0.06	0.53	0.05	0.27	0.73	0.26

[a]TX-1, E-W arm of crossed inverted V wire array 1 (5.255010 MHz); TX-2, N-S arm of crossed inverted V wire array 1 (5.255020 MHz); TX-3, E-W arm of crossed inverted V wire array 2 (5.255030 MHz); TX-4, N-S arm of crossed inverted V wire array 2 (5.255040 MHz); RX-1, vertical whip 1 (N-S arm); RX-2, vertical whip 2 (N-S arm); RX-3, vertical whip 3 (N-S/E-W arms); RX-4, vertical whip 4 (E-W arm); RX-5, vertical whip 5 (E-W arm); RX-6, large loop antenna (E-W orientation); RX-7, N-S arm of crossed inverted V wire array; RX-8, E-W arm of crossed inverted V wire array.

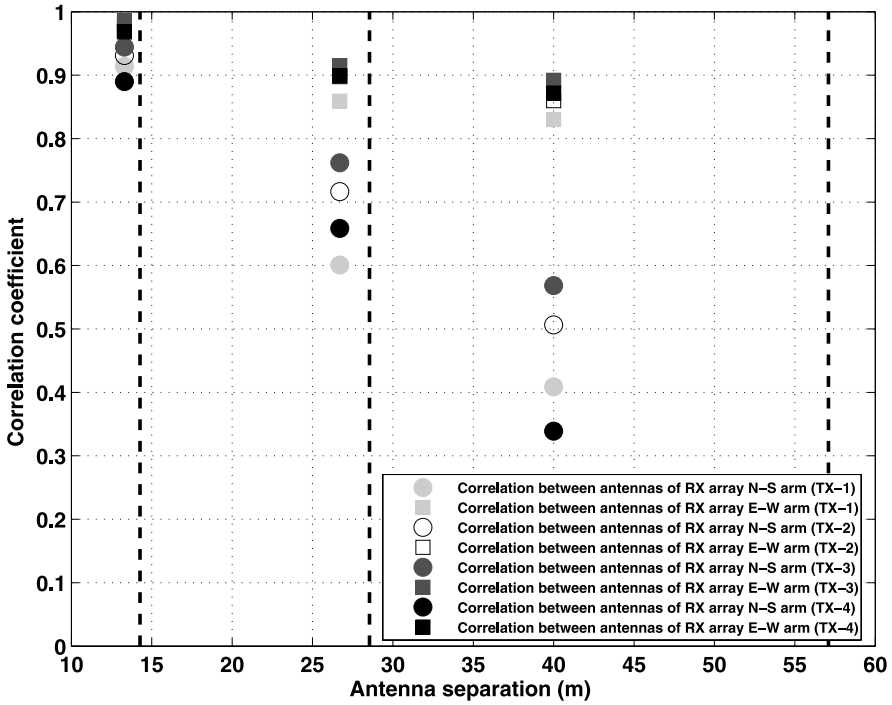

Figure 4. The magnitudes of amplitude correlation coefficients computed for various antenna pair spacings of the L-shaped vertical monopole receiving antenna array for each of the four transmissions at 1602 UT on 2 November 2007. (The data have been divided into two parts depending on the orientation of the particular receiving antenna arm. The vertical dotted lines from right to left represent the distances of one wavelength, half a wavelength, and one quarter of a wavelength, respectively. TX-1, E-W arm of crossed inverted V wire array 1 (5.255010 MHz); TX-2, N-S arm of crossed inverted V wire array 1 (5.255020 MHz); TX-3, E-W arm of crossed inverted V wire array 2 (5.255030 MHz); TX-4, N-S arm of crossed inverted V wire array 2 (5.255040 MHz).)

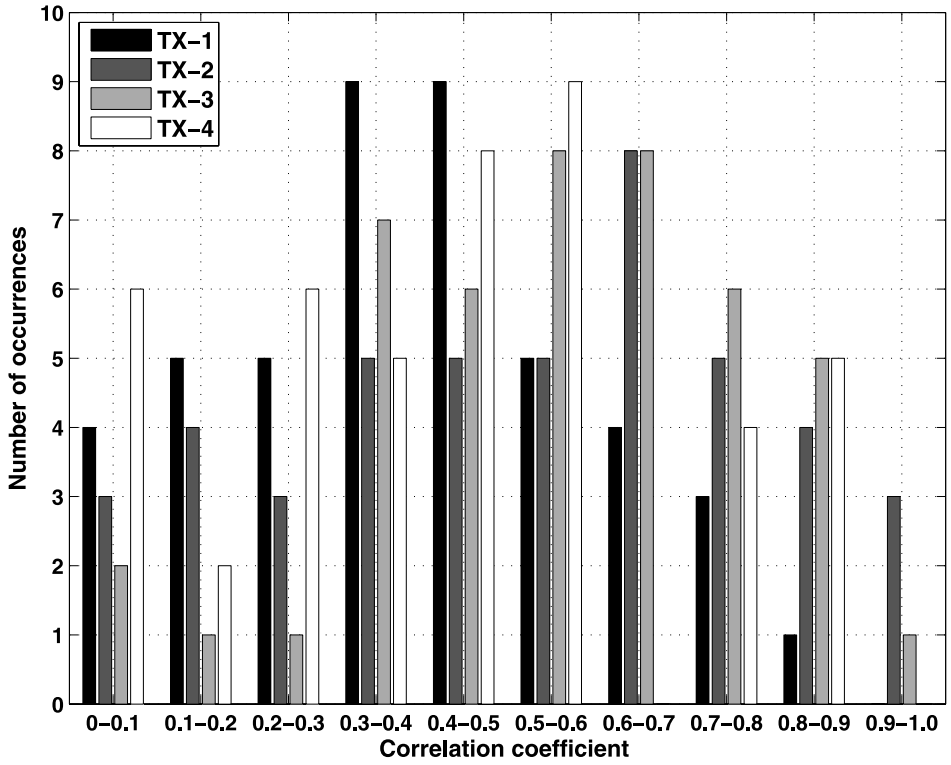

Figure 5. The occurrence frequency histograms of the magnitudes of amplitude correlation coefficients between the N-S and E-W receiving crossed wire antennas for each of the transmitting antennas (45 1-min data files were analyzed). The 4 × 8 MIMO campaign was on 2 November 2007. TX-1, E-W crossed inverted V wire 1 (5.255010 MHz); TX-2, N-S crossed inverted V wire 1 (5.255020 MHz); TX-3, E-W crossed inverted V wire 2 (5.255030 MHz); TX-4, N-S crossed inverted V wire 2 (5.255040 MHz).

from the Chilton (United Kingdom) ionosonde station (located approximately 215 km from the midpoint of the Durham-Bruntingthorpe path at a bearing of 180°), ionospheric conditions supporting multiple propagation modes were confirmed (a typical ionogram transmission curve plot obtained during this campaign is shown in Figure 3). The existence of a strong E region in the ionosphere gave rise to many more modes (1E and 2E) in addition to the 1F and 2F modes (and both the ordinary and extraordinary modes).

3.1.2. Effects of Antenna Spacing and Antenna Orientation on Interelement Correlation at the Transmitter and Receiver

[11] In order to achieve the MIMO capacity, it is essential that there is sufficient decorrelation between the different antenna elements at both ends of the link. In this investigation, the correlation coefficients were computed for various antenna pairs for each data acquisition period (of approximately 1-min duration). Specifically, in this paper, interelement correlation coefficient refers to either (1) the correlation coefficient of signal amplitudes between pairs of transmissions at each receiving antenna or (2) the correlation coefficient of signal amplitudes between pairs of receiving antennas for each individual transmission.

[12] For the typical period of data acquisition presented in Figure 2, the magnitudes of the amplitude correlation coefficients between the individual transmissions at each of the receiving antennas have been listed in Table 1. Expectedly, the orthogonal arms of the transmit crossed wire antennas (i.e., the N-S and E-W oriented wires [TX-1, TX-2], [TX-1, TX-4], [TX-2, TX-3], and [TX-3, TX-4]) exhibit significantly lower levels of correlation compared to the parallel arms ([TX-1, TX-3], [TX-2, TX-4]). This behavior was also observed in other measurements made during this campaign. The resultant correlation coefficients for various antenna pair spacings of the L-shaped array in this example are depicted in Figure 4. In order to identify orientation-dependent fading effects, the data from each transmitter (indicated by the different

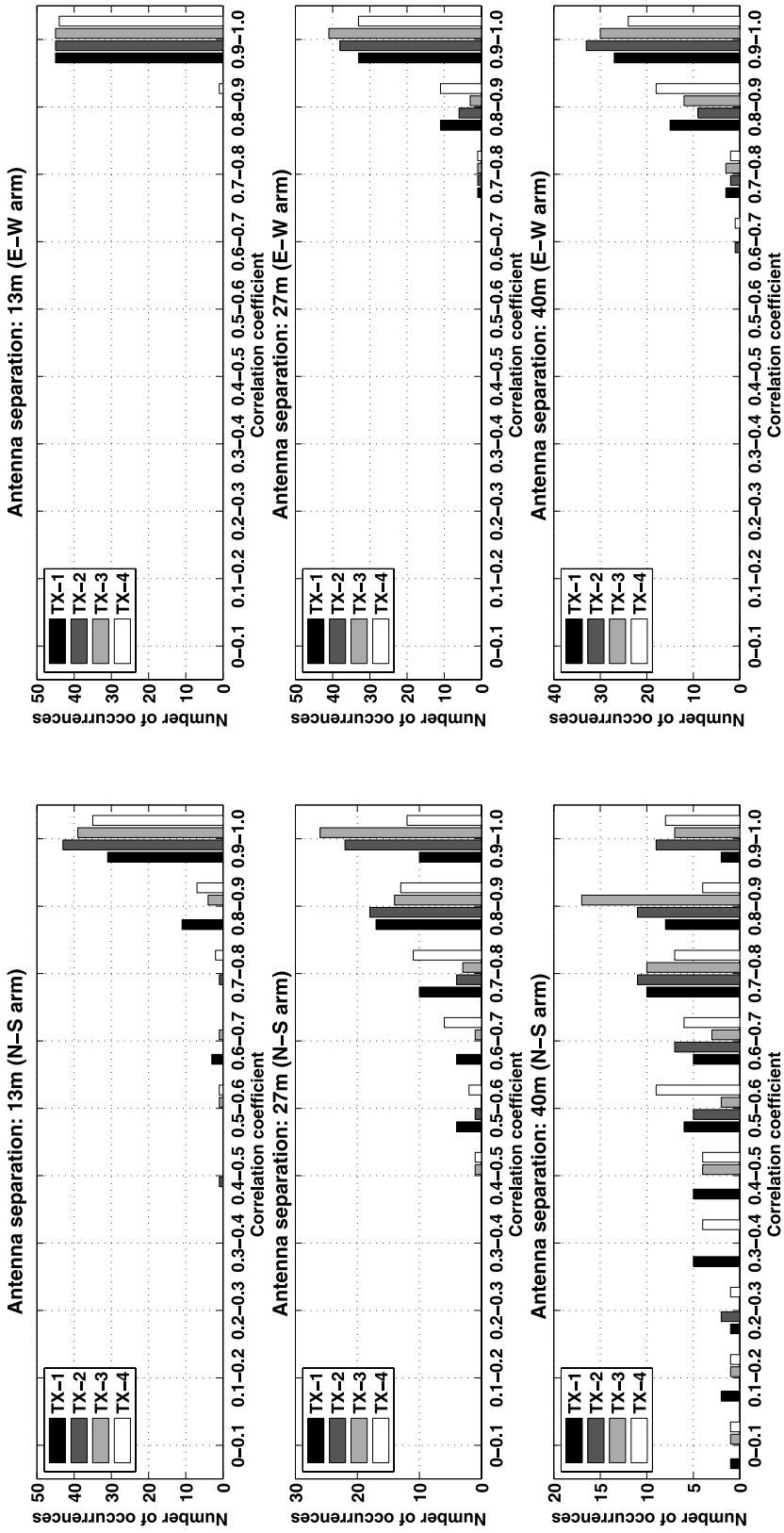

Figure 6. Amplitude correlation coefficient occurrence frequency histograms for various antenna pairs (for separations of 13 m along the N-S arm, 13 m along the E-W arm, 27 m along the N-S arm, 27 m along the E-W arm, 40 m along the N-S arm, and 40 m along the E-W arm) comprising the L-shaped antenna array of vertical whips for each of the transmitting antennas (45 1-min data files were analyzed). The 4 × 8 MIMO campaign was on 2 November 2007. TX-1, E-W arm of crossed inverted V wire array 1 (5.255010 MHz); TX-2, N-S arm of crossed inverted V wire array 1 (5.255020 MHz); TX-3, E-W arm of crossed inverted V wire array 2 (5.255030 MHz); TX-4, N-S arm of crossed inverted V wire array 2 (5.255040 MHz).

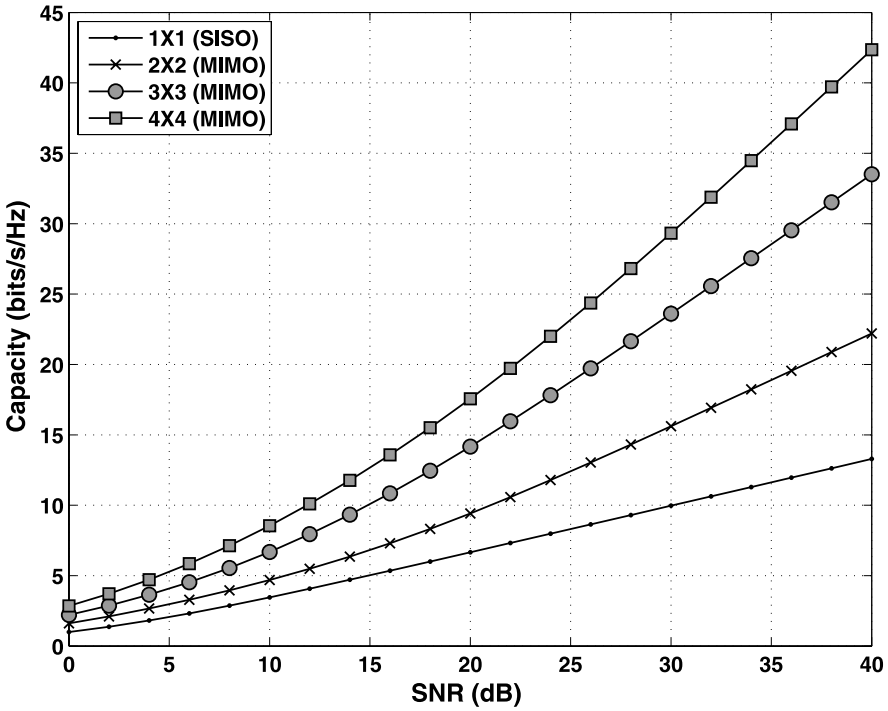

Figure 7. Estimates of channel capacity for various MIMO configurations corresponding to a 1-min data file measured at 1602 UT on 2 November 2007 and evaluated for different signal-to-noise ratios (between 0 and 40 dB).

colors) have been divided into two parts (indicated by the different symbols) depending on the orientation of the particular receiving antenna arm: N-S arm of L-shaped array (circles) and E-W arm of L-shaped array (squares). Figure 4 indicates the occurrence of a strong directional effect. Compared to the E-W arm, the correlation coefficients between different pairs of antennas in the N-S arm of the L-shaped array decrease much more rapidly with antenna separation. Specifically, at the maximum antenna spacing along each arm of 40 m, the values of correlation coefficient for all four transmissions drop to 0.30–0.60. This behavior could be attributed to (1) the orthogonality at the transmit end of the link and/or (2) the fact that along the N-S arm of the L-shaped array, the incoming radio waves would have to travel comparatively different distances (therefore resulting in more decorrelation) compared to the orthogonal E-W arm.

[13] With the receive crossed wire antenna array, the correlation coefficients between the N-S and E-W arms for the 60 s data file collected at 1602 UT are 0.49 (for TX-1), 0.56 (for TX-2), 0.43 (for TX-3), and 0.50 (for TX-4). Figure 5 depicts, for each of the transmissions, the occurrence frequency histograms of the correlation coefficients between the N-S and E-W arms of the receiver crossed wire array (a total 45 1-min data files were analyzed). The majority of correlation coefficients fall within the range 0.3–0.7 indicating that under the prevailing multipath conditions in the ionosphere, the orthogonal orientation of the wire antennas is resulting in sufficient levels of decorrelation to be effective for achieving a MIMO capacity gain (according to *Loyka* [2001], for a 10-element uniform linear array, the MIMO channel capacity does not degrade significantly until the interelement correlation coefficient exceeds approximately 0.9).

[14] The correlation coefficient occurrence frequency histograms for various antenna pairs comprising the L-shaped receiving array are presented in Figure 6 for each of the transmitting antennas (45 1-min data files were analyzed). The histograms illustrate the effect of spatial separation at the receiver: the greater is the separation between receiving antennas, the lower is the correlation between the corresponding amplitude patterns and vice versa. Consequently, at HF wavelengths, the use of homogeneous spaced antenna arrays (such as the L-shaped array) may, at times, require spacing considerably in excess of those employed here to achieve acceptable levels of decorrelation for use in MIMO systems. The histograms also highlight for the complete measurement period, the effect of antenna array orientation at the

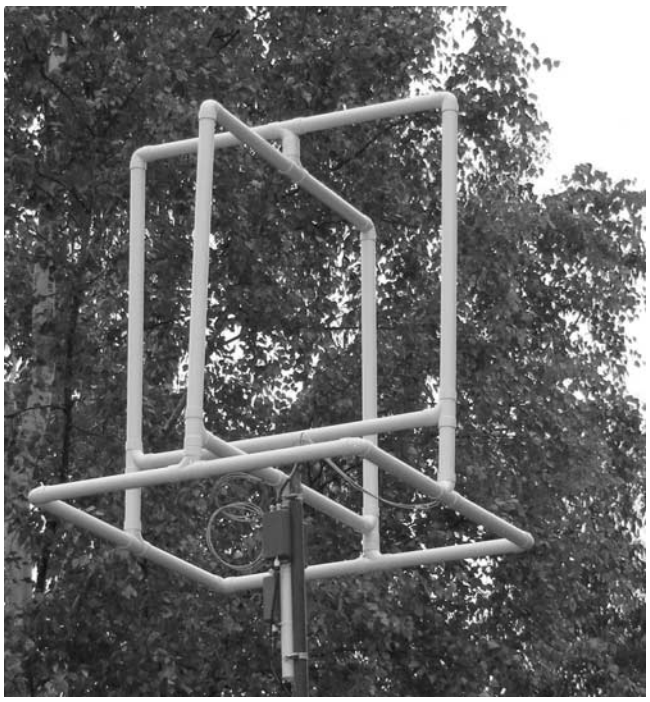

Figure 8. Photograph of three-axis, *H* field active loop antenna array (an example of a compact, heterogeneous antenna array) utilized at the receiver end during some of the HF MIMO experiments.

receiver that was also observed in Figure 4. Particularly at the maximum antenna separation (along each arm of the L-shaped array) of 40 m, the correlation coefficients between the antennas along the N-S arm (i.e., vertical monopoles 1 and 3 in Figure 1) are considerably lower than those along the E-W arm (i.e., vertical monopoles 3 and 5 in Figure 1).

3.1.3. MIMO Capacity Estimation

[15] To quantify the benefit of utilizing a MIMO scheme, the channel capacities (in bits/s/Hz) for various MIMO configurations were estimated using equation (1) [*Razavi-Ghods et al.*, 2004]

$$C = \log_2 \left[\det\left(I_{N_r} + \frac{\rho}{N_t} HH^* \right) \right], \qquad (1)$$

where ρ is the signal-to-noise ratio (SNR), N_t is the number of antennas at the transmitter, N_r is the number of antennas at the receiver, H is the N_rN_t measured complex channel matrix and H^* is the conjugate transpose of this matrix. The entries of the H matrix were calculated using the peaks of the Fourier transform of the received signal. For each MIMO configuration, the complex channel matrix was then normalized using the Frobenius norm as outlined by *Wallace et al.* [2003] and *Razavi-Ghods et al.* [2004].

[16] The capacities were evaluated over a signal-to-noise ratio range of 0–40 dB. Example plots of the channel capacities corresponding to the typical period of data acquisition presented in Figure 2 are shown in Figure 7. It may be noted that for the 4 × 4, 3 × 3, and 2 × 2 systems, data corresponding to the first four transmitting (TX-1, TX-2, TX-3, TX-4) and receiving antennas (RX-1, RX-2, RX-3, RX-4), the first three transmitting (TX-1, TX-2, TX-3) and receiving antennas (RX-1, RX-2, RX-3), and the first two transmitting (TX-1, TX-2) and receiving antennas (RX-1, RX-2), respectively, were utilized to establish the complex channel matrices. For comparison, the Shannon capacities for a single input single output (SISO) have also been plotted in Figure 7. It is evident that there are marked improvements in the MIMO capacities for the 2 × 2, 3 × 3, and 4 × 4 systems over that of the SISO system. For example, at an SNR of 30 dB, the SISO system yields a capacity of approximately 10 bits/s/Hz while the 2 × 2, 3 × 3, and 4 × 4 MIMO systems result in capacities of 15.6 bits/s/Hz, 23.6 bits/s/Hz and 29.3 bits/s/Hz, respectively. Similar improvements in capacity were observed in the other measurements. It may be noted that the wideband capacity can be obtained by taking the average capacity of a number of carriers in the given bandwidth. This, on average, can result in a higher-capacity estimate

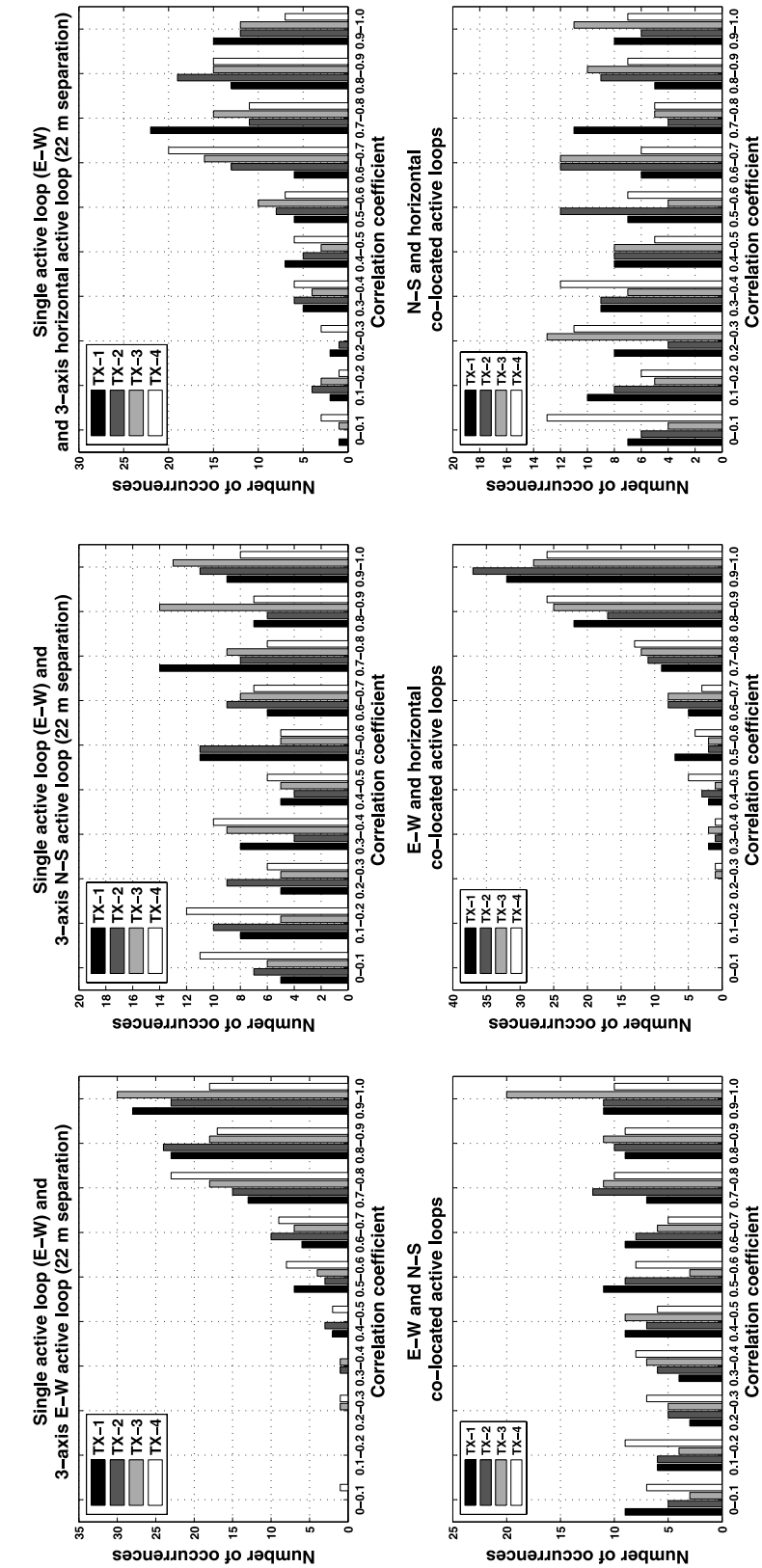

Figure 9. The occurrence frequency histograms of the magnitudes of amplitude correlation coefficients between the various pairs of receiving antennas for each of the transmitting antennas (79 1-min data files were analyzed). The 4×4 MIMO campaign was on 3 September 2008. TX-1, N-S arm of crossed inverted V wire array (5.255010 MHz); TX-2, E-W arm of crossed inverted V wire array (5.255020 MHz); TX-3, diamond-shaped loop antenna (5.255030 MHz); TX-4, vertical whip antenna (5.255040 MHz).

Table 2. Mean Values of the Amplitude Correlation Coefficients Between Perpendicular Pairs of Receiving Antennas Comprising the Colocated Active Loop Array for Each of the Transmitting Antennas[a]

Receiving Antenna Pairs Being Correlated	Transmitter	Mean Correlation Coefficient
E-W and N-S colocated active loops	TX-1	0.54
	TX-2	0.58
	TX-3	0.65
	TX-4	0.53
E-W and horizontal colocated active loops	TX-1	0.82
	TX-2	0.84
	TX-3	0.82
	TX-4	0.81
N-S and horizontal colocated active loops	TX-1	0.49
	TX-2	0.51
	TX-3	0.54
	TX-4	0.45

[a]The mean values are from over the whole measurement period. Here 79 1-min data files were analyzed. The 4 × 4 MIMO campaign was on 3 September 2008. TX-1, N-S arm of crossed inverted V wire array (5.255010 MHz); TX-2, E-W arm of crossed inverted V wire array (5.255020 MHz); TX-3, diamond-shaped loop antenna (5.255030 MHz); TX-4, vertical whip antenna (5.255040 MHz).

than the single carrier capacity because of the frequency diversity gain. Finally, it was also observed that, in general, as the levels of decorrelation between pairs of antennas increased, there was a corresponding improvement in the estimated channel capacity and vice versa.

3.2. The 4 × 4 MIMO Configuration (3 September 2008)

[17] Between July and September 2008, several experimental campaigns were conducted in order to investigate the feasibility of utilizing colocated, heterogeneous antenna arrays at the receiver. For this purpose, a three-axis, *H* field loop antenna array was designed that consisted of three orthogonal active square loop antennas (each of side length ∼1 m) mounted on a common mast (of height ∼3 m), two antennas oriented in the E-W (RX-2) and N-S (RX-3) directions and a horizontal loop antenna (RX-4) (Figure 8). On 3 September 2008, a measurement campaign was conducted that employed this antenna array at the receive end of a 4 × 4 MIMO link. A single active square loop antenna (side length ∼ 1 m) oriented in the E-W direction and mounted 2 m above ground level was also deployed at the receiver (RX-1) at a distance of approximately 22 m from the heterogeneous array.

[18] To examine the effects of antenna heterogeneity at the transmit end, the following four different antennas were utilized in Durham with a nominal frequency of 5.2550 MHz: TX-1 (5.255010 MHz), N-S arm of an inverted V wire antenna array (i.e., pointing in the direction of Bruntingthorpe); TX-2 (5.255020 MHz), E-W arm of an inverted V wire antenna array; TX-3 (5.255030 MHz), diamond-shaped commercial portable loop antenna (side length ∼1 m); and TX-4 (5.255040 MHz), vertical whip antenna. The geometry of the orthogonally oriented inverted V wire antennas was identical to that used in the campaign described in section 3.1. The loop was approximately 8 m east and 2 m south of the central mast of the inverted V antennas. The vertical antenna was located approximately 15 m west and 2 m south of the central mast of the inverted V antennas.

3.2.1. Structure of the Ionosphere and Fading

[19] During this measurement campaign, deep fading occurred on all four receiving antennas for majority of the measurements. The corresponding Chilton vertical ionogram transmission curve plots once again denoted the presence of a number of multipath components during the acquisition period: the ordinary and extraordinary modes for the 1*F* and 2*F* paths were present along with multiple components from *E* region reflections as well.

3.2.2. Effects of Antenna Spacing and Antenna Heterogeneity on Interelement Correlation at the Transmitter and Receiver

[20] The occurrence frequency histograms of the correlation coefficients between the various pairs of receiving antennas for each of the transmitting antennas are presented in Figure 9 (79 1-min data files were analyzed). The lower three frames depict the histograms of the correlation coefficients between the various pairs of orthogonal loop antennas comprising the colocated, three-axis loop array. In particular, for the perpendicular pairs involving the N-S oriented active loop, sufficiently low levels of correlation coefficient are observed for all four transmissions, indicating that despite being colocated, the heterogeneous nature of the three loops is effective in facilitating the necessary decorrelation in the MIMO system. Over the whole measurement period, the mean values of the correlation coefficients between the perpendicular loops do not exceed 0.85 for any of the transmissions (these have been listed in Table 2).

[21] The top frame in Figure 9 contains the occurrence frequency histograms of the correlation coefficients between the single active loop antenna (oriented in the E-W direction) and each of the loop antennas comprising the colocated, heterogeneous array (located at a distance of approximately 22 m from the single active loop). In general, the spatial separation is producing reasonably low values of correlation coefficient for all three antenna pairs, including the parallel oriented loops (i.e., single E-W loop and E-W colocated loop). However, as expected, the additional orthogonality that the single E-W loop has with respect to the N-S colocated loop and the horizontal colocated loop is producing further decorrelation (the distances between the single E-W loop and all three active loops of the colocated array are identical).

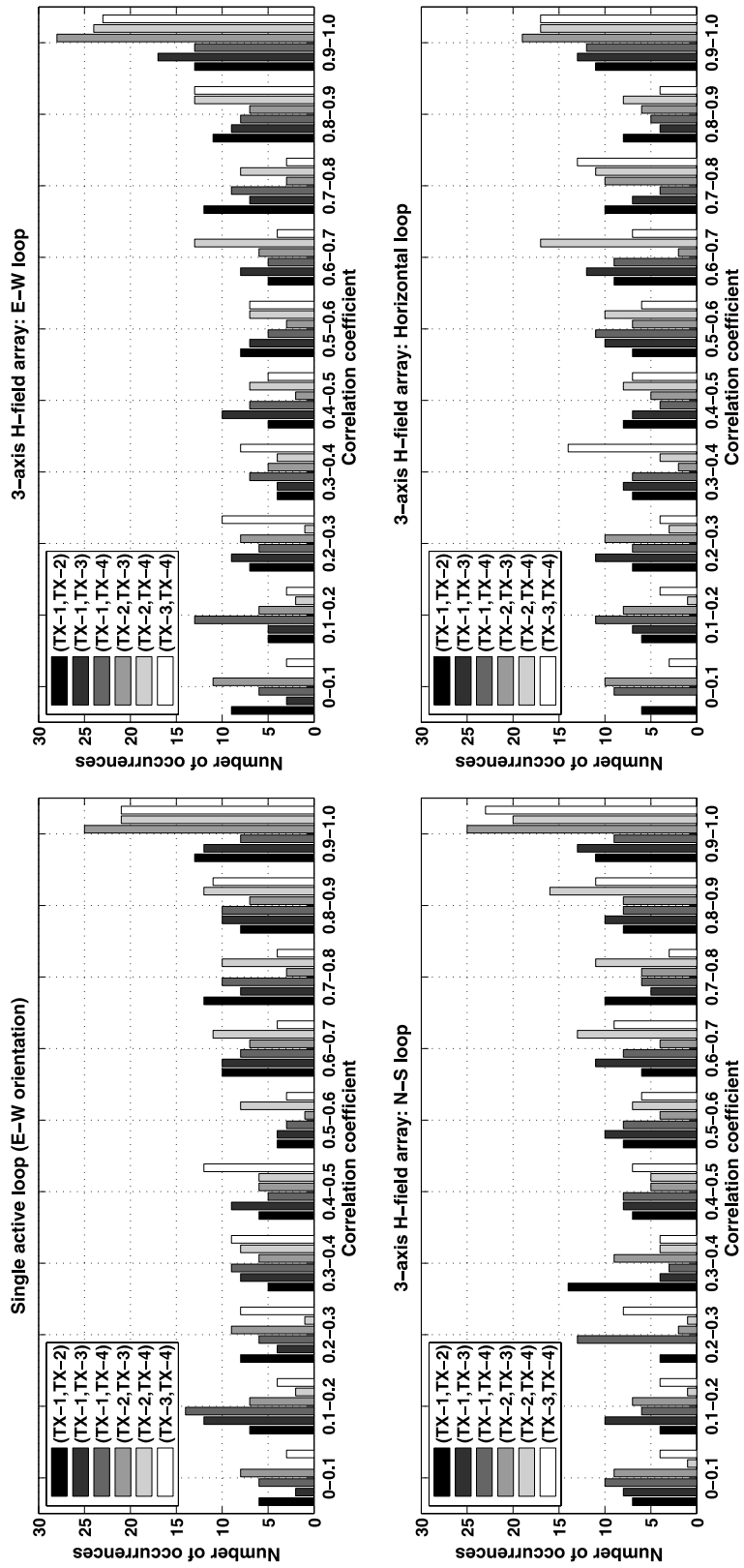

Figure 10. The occurrence frequency histograms of the magnitudes of amplitude correlation coefficients between the various pairs of transmitting antennas at each of the receiving antennas (79 1-min data files were analyzed). The 4×4 MIMO campaign was on 3 September 2008. TX-1, N-S arm of crossed inverted V wire array (5.255010 MHz); TX-2, E-W arm of crossed inverted V wire array (5.255020 MHz); TX-3, diamond-shaped loop antenna (5.255030 MHz); TX-4, vertical whip antenna (5.255040 MHz).

Table 3. Mean Values of the Amplitude Correlation Coefficients Between Various Pairs of Transmitting Antennas at Each of the Receiving Antennas[a]

Transmitting Antenna Pairs Being Correlated	Receiver	Mean Correlation Coefficient
(TX-1, TX-2)	Single active loop antenna (E-W orientation)	0.56
(TX-1, TX-3)	Single active loop antenna (E-W orientation)	0.56
(TX-1, TX-4)	Single active loop antenna (E-W orientation)	0.51
(TX-2, TX-3)	Single active loop antenna (E-W orientation)	0.58
(TX-2, TX-4)	Single active loop antenna (E-W orientation)	0.70
(TX-3, TX-4)	Single active loop antenna (E-W orientation)	0.61
(TX-1, TX-2)	Colocated, three-axis, *H* field antenna array (E-W loop)	0.57
(TX-1, TX-3)	Colocated, three-axis, *H* field antenna array (E-W loop)	0.60
(TX-1, TX-4)	Colocated, three-axis, *H* field antenna array (E-W loop)	0.52
(TX-2, TX-3)	Colocated, three-axis, *H* field antenna array (E-W loop)	0.59
(TX-2, TX-4)	Colocated, three-axis, *H* field antenna array (E-W loop)	0.73
(TX-3, TX-4)	Colocated, three-axis, *H* field antenna array (E-W loop)	0.64
(TX-1, TX-2)	Colocated, three-axis, *H* field antenna array (N-S loop)	0.55
(TX-1, TX-3)	Colocated, three-axis, *H* field antenna array (N-S loop)	0.56
(TX-1, TX-4)	Colocated, three-axis, *H* field antenna array (N-S loop)	0.49
(TX-2, TX-3)	Colocated, three-axis, *H* field antenna array (N-S loop)	0.60
(TX-2, TX-4)	Colocated, three-axis, *H* field antenna array (N-S loop)	0.73
(TX-3, TX-4)	Colocated, three-axis, *H* field antenna array (N-S loop)	0.64
(TX-1, TX-2)	Colocated, three-axis, *H* field antenna array (horizontal loop)	0.55
(TX-1, TX-3)	Colocated, three-axis, *H* field antenna array (horizontal loop)	0.56
(TX-1, TX-4)	Colocated, three-axis, *H* field antenna array (horizontal loop)	0.49
(TX-2, TX-3)	Colocated, three-axis, *H* field antenna array (horizontal loop)	0.54
(TX-2, TX-4)	Colocated, three-axis, *H* field antenna array (horizontal loop)	0.68
(TX-3, TX-4)	Colocated, three-axis, *H* field antenna array (horizontal loop)	0.59

[a]The mean values are from over the whole measurement period. Here 79 1-min data files were analyzed. The 4×4 MIMO campaign was on 3 September 2008. TX-1, N-S arm of crossed inverted V wire array (5.255010 MHz); TX-2, E-W arm of crossed inverted V wire array (5.255020 MHz); TX-3, diamond-shaped loop antenna (5.255030 MHz); TX-4, vertical whip antenna (5.255040 MHz).

[22] The occurrence frequency histograms of the correlation coefficients between the individual transmissions at each of the receiving antennas are presented in Figure 10. The plots indicate that under the prevailing ionospheric propagation conditions, as a consequence of the antenna heterogeneity at the transmit end of the link, the magnitudes of the amplitude correlation coefficients between the transmitting elements are appreciably low at all four receiving antennas. The mean values (over the whole measurement period) of the correlation coefficients between the various transmitting antennas at each of the receiving antennas are listed in Table 3 and are observed to never exceed 0.75.

3.2.3. MIMO Capacity Estimation

[23] Plots of the average channel capacity for various MIMO configurations corresponding to all the data collected during the measurement campaign (79 1-min data files) and evaluated for different signal-to-noise ratios (between 0 and 40 dB) are presented in Figure 11. From the graph, it is observed that there are distinct improvements in the MIMO capacities for the 2×2, 3×3, and 4×4 systems over that of the Shannon SISO system. Furthermore, despite using colocated antennas at the receiver end, the channel capacities obtained are very similar to the channel capacities acquired with the configuration employing spaced antennas at the receiver. Therefore, under suitable ionospheric conditions, colocated heterogeneous arrays (as opposed to traditional homogeneous spaced arrays like the L-shaped array described in sections 2 and 3.1) will significantly reduce the amounts of space required at both ends of a radio link. With the relatively long wavelengths involved in the HF band, this is particularly suitable for applications where the deployment of large, spaced arrays is not appropriate.

4. Concluding Remarks

[24] For a MIMO system to successfully produce increased channel capacities, it is essential that there is sufficient decorrelation between the signals received at each of the antenna elements of the receiver array from each of the elements of the transmitter array. As confirmed in this analysis, at HF, depending on the prevailing modal structure of the ionosphere, the use of homogeneous spaced arrays may require significant spacing to achieve acceptable levels of decorrelation. Decorrelation effects that are distinctly orientation dependent have also been observed both in the context of spaced arrays as well as colocated, heterogeneous arrays.

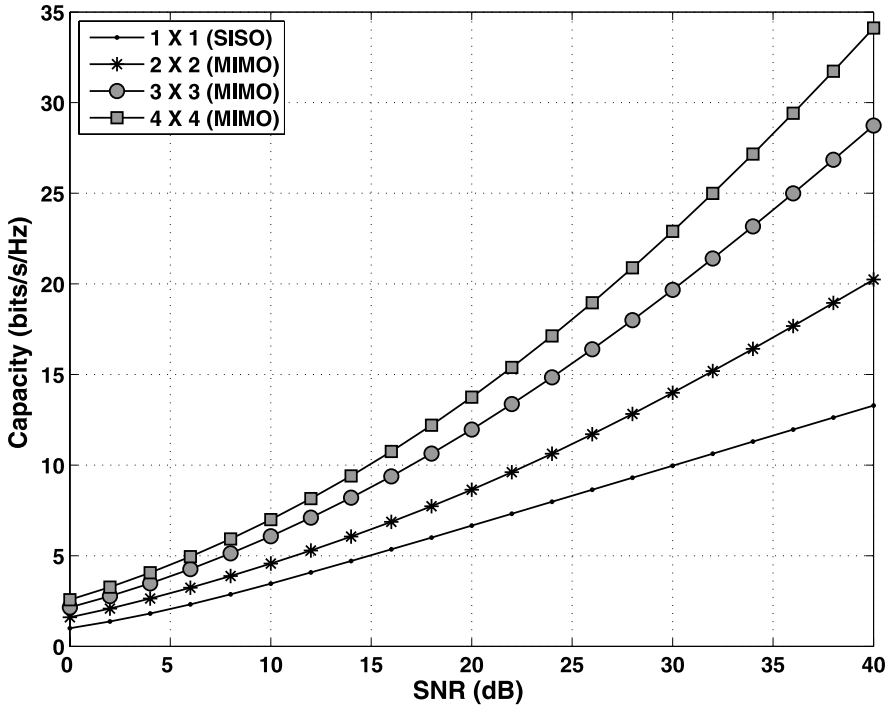

Figure 11. Plots of the average channel capacity for various MIMO configurations corresponding to data from a measurement campaign conducted on 3 September 2008 (79 1-min data files were analyzed) and evaluated for different signal-to-noise ratios (between 0 and 40 dB).

For example, at times the two orthogonal arms of a spaced L-shaped antenna array of vertical monopoles exhibit significantly different levels of decorrelation (as a function of antenna spacing). Moreover, in most of the experimental campaigns conducted, antenna heterogeneity at the transmit end of the link has resulted in low values of interelement correlation coefficient.

[25] This paper has presented preliminary yet significant results in the context of using compact, heterogeneous antenna arrays at the receiving end of HF MIMO links. Specifically, a colocated, heterogeneous loop antenna array consisting of three orthogonally oriented loops is effective in facilitating the necessary decorrelation required in a MIMO system. Looking to the future, the use of colocated, heterogeneous antenna arrays at the transmitter will also be investigated. IETR, Rennes University specializes in the design of compact, colocated as well as spaced, heterogeneous antenna arrays [*Erhel et al.*, 2004; *Perrine et al.*, 2004]. Experiments will be conducted with the various IETR antenna configurations available at Rennes. Another compact, three-channel, heterogeneous receiving antenna array is currently being constructed at the Universities of Leicester and Durham, the configuration of which is based on the design of a unique ground symmetric loop antenna system developed by *Massie et al.* [2004].

[26] The receiver system will also be deployed in northern Scandinavia in order to obtain measurements over a path with different, more disturbed, propagation characteristics. Finally, a measurement system using state of the art digital synthesis techniques is being designed that will permit both narrowband and wideband measurements to be made in the future. In particular, the waveform generator will employ a direct digital frequency synthesizer that will facilitate the generation of a wide range of waveforms including CW signals with fine tuning, a modulated pseudo random binary sequence and chirp waveforms.

[27] **Acknowledgments.** The authors are grateful to the EPSRC for their financial support of this work. They would also like to thank the UK Solar System Data Centre for provision of data from the Chilton ionosonde. Collaboration between the United Kingdom and French groups in this investigation was facilitated through the EU COST-296 Action on the Mitigation of Ionospheric Effects on Radio Systems (MIERS).

References

Brine, N. L., C. C. Lim, A. D. Massie, and W. Marwood (2006), Capacity estimation for the HF-MIMO channel, paper presented at Sixth Symposium on Radiolocation and Direction Finding, Southwest Res. Inst., San Antonio, Tex.

Erhel, Y., D. Lemur, L. Bertel, and F. Marie (2004), HF radio direction finding operating on a heterogeneous array: Principles and experimental validation, *Radio Sci.*, *39*, RS1003, doi:10.1029/2002RS002860.

Foschini, G. J. (1996), Layered space-time architecture for wireless communication in a fading environment when using multi-element antennas, *Bell Lab. Tech. J.*, *1*(2), 41–59, doi:10.1002/bltj.2015.

Gesbert, D., H. Bolskei, D. A. Gore, and A. J. Paulraj (2002), Outdoor MIMO wireless channels: Models and performance prediction, *IEEE Trans. Commun.*, *50*(12), 1926–1934, doi:10.1109/TCOMM.2002.806555.

Gunashekar, S. D., E. M. Warrington, S. Salous, S. M. Feeney, H. Zhang, N. Abbasi, L. Bertel, D. Lemur, and M. Oger (2008), Early results of experiments to investigate the feasibility of employing MIMO techniques in the HF band, paper presented at Loughborough Antennas and Propagation Conference 2008, Loughborough Univ., Loughborough, U. K.

Lim, H. M., C. C. Constantinou, and T. N. Arvanitis (2007), On the ensemble average capacity of multiple-input multiple-output channels in outdoor line-of-sight multipath urban environments, *Radio Sci.*, *42*, RS1006, doi:10.1029/2005RS003406.

Loyka, S. L. (2001), Channel capacity of MIMO architecture using the exponential correlation matrix, *IEEE Commun. Lett.*, *5*(9), 369–371, doi:10.1109/4234.951380.

Massie, A., W. Martinsen, D. Taylor, M. Chamalaun, and J. Sorensen (2004), GISELLE–DF using phase data from a ground symmetric loop, paper presented at Fifth Symposium on Radiolocation and Direction Finding, Southwest Res. Inst., San Antonio, Tex.

Perrine, C., Y. Erhel, D. Lemur, L. Bertel, and A. Bourdillon (2004), A way to increase the bit rate in ionospheric radio links, *Ann. Geophys.*, *47*(2/3), 1145–1160.

Razavi-Ghods, N., M. Abdalla, and S. Salous (2004), Characterisation of MIMO propagation channels using directional antenna arrays, paper presented at Fifth International Conference on 3G Mobile Technologies, Ind. Electron. Eng., London.

Salous, S., E. M. Warrington, S. D. Gunashekar, S. M. Feeney, N. Abbasi, H. Zhang, L. Bertel, D. Lemur, and M. Oger (2008), MIMO Channel Measurements in the HF Band, paper presented at 2008 General Assembly, Int. Union of Radio Sci., Chicago, Ill.

Shiu, D.-S., G. J. Foschini, M. J. Gans, and J. M. Kahn (2000), Fading correlation and its effect on the capacity of multi-element antenna systems, *IEEE Trans. Commun.*, *48*(3), 502–513, doi:10.1109/26.837052.

Strangeways, H. J. (2006), Estimation of signal correlation at spaced antennas for multi-moded ionospherically reflected signals and its effect on the capacity of SIMO and MIMO HF links, paper presented at 10th International Conference on Ionospheric Radio Systems and Techniques 2006, Inst. of Eng. and Technol., London.

Wallace, J. W., M. A. Jensen, A. L. Swindlehurst, and B. D. Jeffs (2003), Experimental characterization of the MIMO wireless channel: Data acquisition and analysis, *IEEE Trans. Wireless Comm.*, *2*(2), 335–343, doi:10.1109/TWC.2003.808975.

Xu, S., H. Zhang, H. Yang, and H. Wang (2004), New considerations for high frequency communications, paper presented at 10th Asia-Pacific Conference on Communications and 5th International Symposium on Multi-Dimensional Mobile Communications, Inst. of Electr. And Electron. Eng., Beijing.

N. M. Abbasi, S. D. Gunashekar, and E. M. Warrington, Department of Engineering, University of Leicester, University Road, Leicester LE1 7RH, UK. (emw@le.ac.uk)

L. Bertel, D. Lemur, and M. Oger, IETR, UMR6164, Université de Rennes 1, CNRS, F-35042 Rennes, France.

S. M. Feeney and S. Salous, School of Engineering, Durham University, South Road, Durham DH1 3LE, UK.